SIDEROPHILE ELEMENT CONCENTRATIONS IN BENCUBBINITE METALS. A. J. Campbell[1], M. Humayun[1], and M. K. Weisberg[2], [1]Dept. of the Geophysical Sciences, University of Chicago, Chicago, IL 60637, USA (acampbel@midway.uchicago.edu), [2]Dept. of Physical Sciences, Kingsborough College CUNY, Brooklyn, NY 11235, USA.

Introduction: Bencubbinites (CB chondrites) are primitive, metal-rich breccias that are closely related to the CR and CH chondrites [1]. Bencubbinite metal occurs as three types: as large sulfide-bearing aggregates, as homogeneous sulfide-free grains, and as sulfide-free grains that are zoned in Ni and other siderophiles [1]. Zoned metal in the bencubbinites QUE94411 and Hammadah al Hamra 237 was previously analyzed for platinum group element (PGE) distributions, and it was found that these zoned siderophile element patterns support a condensation origin for the siderophile element enrichments in the cores of the zoned metal grains [2, 3]. The unzoned metal in bencubbinites exhibits a positive Ni-Co correlation that has also been interpreted to result from a nebular condensation process [1, 4]. We have tested the proposed condensation origin of unzoned bencubbinite metal by measuring trace siderophile element abundances in both metal aggregates and homogeneous grains.

Experimental: Polished slabs of Bencubbin, Weatherford, Gujba, and Hammadah al Hamra 237 were examined optically and by SEM. Grain sizes ranged from ~100 μm for unaggregated, homogeneous metal in HH237 to several mm for metal aggregates in Bencubbin, Weatherford, and Gujba. Nickel concentrations at the cores and rims of metal grains were measured by EDX to determine whether the metal was zoned. Zoned metal was not found in Bencubbin, Weatherford, or Gujba. Unzoned metal grains in each section were selected for trace siderophile element analysis by LA-ICP-MS. A CETAC LSX-200 laser ablation peripheral was used with a magnetic sector ICP mass spectrometer, the Finnigan Element™ [2]. Each point analysis on the sample produced a pit 25-150 μm in diameter and 15-35 μm deep. On large (mm-sized) aggregates, the laser was rastered over the sample during data collection. The isotopes ^{31}P, ^{34}S, ^{53}Cr, ^{57}Fe, ^{59}Co, ^{60}Ni, ^{63}Cu, ^{69}Ga, ^{74}Ge, ^{75}As, ^{95}Mo, ^{101}Ru, ^{103}Rh, ^{105}Pd, ^{118}Sn, ^{121}Sb, ^{182}W, ^{185}Re, ^{192}Os, ^{193}Ir, ^{195}Pt, and ^{197}Au were monitored during some or all of the measurements. Instrumental sensitivity factors for each isotope were determined by measuring signal intensity from metal standards which have known concentrations of the elements of interest [2]. Precision of the LA-ICP-MS measurements varied with spot size and was typically 5-20% (2σ).

Results and Discussion: Siderophile element vs. Ni trends in Gujba are very similar to those observed in Bencubbin (Figure 1), strengthening the assignment of Gujba as a bencubbinite [5]. The lone metal aggregate that we have analyzed for Weatherford plots similarly to the Bencubbin-Gujba trend, although the refractory siderophile concentration in this Weatherford sample is slightly higher. We conclude that the metal in these three meteorites is related and refer to it here as BGW metal. The metal aggregates in HH237 also plot along the BGW trend, although with primarily subchondritic Ni compositions (Figure 1).

Palladium measurements were critical to verifying that the zoned metal grains had a high-temperature condensation origin, because Pd is strongly siderophile and has a volatility similar to that of Fe [2]. The observed lack of Pd zoning in the zoned metal of QUE94411 and HH237 ruled out redox processes as a cause of the zoning [2, 3]. The Pd-Ni trend exhibited by BGW metal in Figure 1, however, has a strongly positive slope that is inconsistent with condensation at presumed nebular pressures (~10 Pa). The Fe, CI-normalized Pd-Ni trend passes through the chondritic composition and has a slope slightly steeper than 1.0 (where a slope of 1.0 would result from addition/subtraction of Fe during reduction/oxidation). The metal aggregates in HH237 plot along the BGW Pd-Ni trend, primarily at near-chondritic and subchondritic Pd/Fe and Ni/Fe ratios.

Unaggregated, homogeneous metal in HH237 has a wider range of Pd/Fe and Ni/Fe values (Figure 1). Some of this metal has compositions consistent with those of the aggregates, while other grains plot well off this trend. Several of the homogeneous metal grains in HH237 have Pd and Ni compositions similar to the zoned metal grains, suggesting a possible condensation origin for these grains.

The refractory PGEs (Ru, Rh, Os, Ir, Pt) correlate positively with Ni in BGW metal, along a trend passing through chondritic PGE/Fe and Ni/Fe ratios. Iridium values are representative of this group of elements and are plotted in Figure 1. The metal aggregates in HH237 also plot along this trend, extending to subchondritic Ir/Fe and Ni/Fe values.

The Fe, CI-normalized Ir/Ni ratio in the most Ni-rich BGW metal is significantly greater than 1.0 (~1.5), which precludes formation of this metal by simple removal and/or addition of Fe during oxidation/reduction of a chondritic precursor. This slope is also steeper than the calculated condensation trajectory [2]; like Pd, the refractory PGEs do not support a condensation origin for metal in Bencubbin, Gujba, and Weatherford.

In the large metal aggregates in Bencubbin, Gujba, and Weatherford, the CI-normalized X/Fe ratios for Ga, Ge, As, Sn, and Sb ranged from 0.01-0.07, 0.001-0.01, 0.2-0.6, 0.01-0.02, and 0.04-0.09, respectively. These low concentrations of moderately volatile siderophiles are consistent with the normalized whole rock abundances that have been previously reported [1].

The trace siderophile element data can be used to eliminate the following origins for the BGW metal: 1) condensation from the solar nebula; 2) oxidation of an initially chondritic composition, leading to loss of Fe; 3) equilibration with a S-rich partial melt. The first two have been discussed above and were rejected because the observed PGE distributions were inconsistent with the expected compositional trends. At low degrees of partial melting and high S contents of the melt, Ni becomes a compatible element, and models can be constructed in which a positive correlation exists between Ni and Ir or Pd [6]. However, under these conditions we find that other important constraints (e.g., the chondritic Co/Ni ratio) are violated, and therefore a partial melt origin may also be rejected as the cause of the trace element signatures of the BGW metal. Having ruled out the above explanations, the cause for the observed fractionation trends in BGW metal is being further investigated.

The metal aggregates in HH237 have trace element abundances similar to the metal in Bencubbin, Gujba, and Weatherford, although the HH237 aggregates extend further to subchondritic compositions (Figure 1). This supports a linked origin for these metals. The unaggregated, homogeneous metal in HH237 is scattered more widely across the plots in Figure 1, and may reflect multiple formation mechanisms for this material. It has been suggested that this metal may have formed by fragmentation of previous aggregates or zoned grains [7]. As indicated above, PGE data for some of the homogeneous grains is similar to that of the zoned grains. However, there is an important difference in Fe, CI-normalized W abundances between the homogeneous grains in HH237 and the BGW metal; most of the homogeneous HH237 metal has subchondritic W/Fe (median = 0.38), whereas most of the BGW metal grains, plus the HH237 aggregates, have superchondritic W/Fe (median = 1.73). Therefore it is unlikely that much of the homogeneous metal in HH237 is a simple fragmentation product of the bencubbinite aggregates. Further, the W variations in bencubbinite metal show none of the systematics observed in the kamacite in equilibrated ordinary chondrites, where W/Ir correlates with Re/Ir [8].

References: [1] Weisberg M. K. et al. (2000) *LPSC XXXI*, #1466; Weisberg M. K. et al. (2000) *MAPS*, submitted. [2] Campbell A. J. et al. (2001) *GCA*, *65*, 163-180. [3] Campbell A. J. et al. (2000) *MAPS*, *35*, A38. [4] Newsom H. E. and Drake M. J. (1979) *GCA*, *43*, 689-707. [5] Rubin A. E. et al. (2001) this volume. [6] Jones J. H. and Malvin D. J. (1990) *Metall. Trans. B*, *21B*, 697-706. [7] Meibom A. (2001) pers. comm. [8] Humayun M. and Campbell A. J. (2001) this volume.

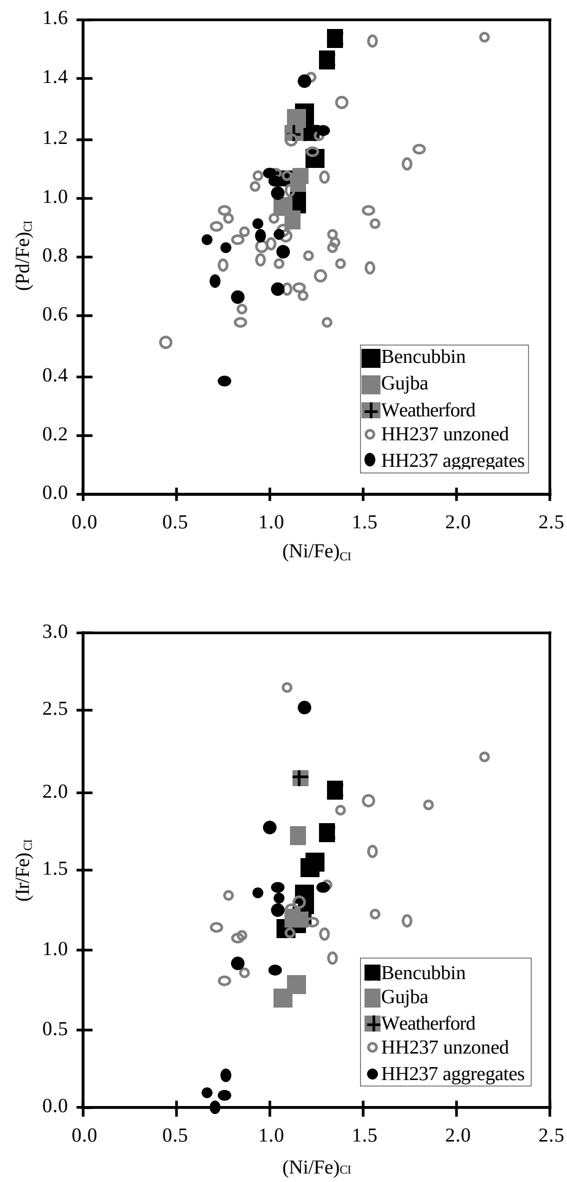

Figure 1. CI-normalized Pd/Fe (top) and Ir/Fe (bottom) ratios plotted against normalized Ni/Fe.